Multipacting simulation and analysis of a taper quarter wave cavity by using Analyst-PT3P*

ZHANG Cong(张聪)[1,2;1)] HE Yuan(何源)[1]
ZHAO Hong-Wei(赵红卫)[1] ZHANG Sheng-Hu(张生虎)[1]

[1] Institute of Modern Physics, Chinese Academy of Sciences, Lanzhou 730000, China
[2] Graduate University of Chinese Academy of Sciences, Beijing 100049, China

Abstract: Since the tapered quarter wave resonator (QWR) cavity is proven to have a much lower peak surface magnetic field in the short plate and a lower peak surface electric field near the beam tube compared with the straight outer conductor QWR, it has been recommended for the separated sector cyclotron linac injector system in the heavy ion research facility in Lanzhou. This paper is focused on the multipacting (MP) analysis for the tapered QWR with a frequency of 80.5 MHz and beta of 0.085. Using the Analyst program, MP bands can be simulated and analyzed with the Particle Tracking module to identify potential problems in the cavity design. This paper will present the simulation results of MP for the tapered QWR cavity.

Key words: multipacting, tapered QWR superconducting cavity, Analyst program

PACS: 29.20.Ej **DOI:** 10.1088/1674-1137/36/4/012

1 Introduction

Multipacting (MP) is a resonant process in radio frequency structures [1]. When it happens, a number of electrons will cost radio frequency power and forbid the increase of cavity fields by just raising the incident power. The electrons impact the cavity walls, leading to a large rise of temperature, and this is critical for superconducting material because it may quench the cavity. Although MP is no longer a big issue for modern cavities of high β, MP is still a problem for low β cavities.

A tapered quarter wave resonator (QWR) cavity working at 80.5 MHz and beta of 0.085 was designed for the linac injector system [2], and MP simulations were done for this cavity to examine whether MP would be an obstacle during the operation. In many cases, we also need to know the potential MP barriers for the higher modes in QWR, because the higher modes help us to check the cavity performance roundly. The simulation results will be reported and analyzed in this paper.

2 Cavity model and field distributions for the fundamental mode and two higher modes

We use the fundamental mode of the cavity to accelerate the beams, however, sometimes during the vertical testing, we also need to check the performance of the higher modes of the cavity, mainly the $3\lambda/4$ and the $5\lambda/4$ modes. Therefore, in this paper, the field distributions of the three modes (one fundamental mode and two higher modes) and MP simulation will be discussed.

Figure 1 shows the schematic diagram of the QWR cavity, the outer conductor has a conical top part which functions to improve the effective shunt impedance R_{a}/Q_0 and decrease the peak surface fields: the peak surface electric field-E_{peak} and the

---

Received 31 May 2011
* Supported by National Nature Science Foundation of China (91026001)

1) E-mail: afeng.cong@gmail.com

Table 1. The electromagnetic figures of merit of the tapered QWR.

mode	frequency/MHz	stored energy/J	E_{peak} /(MV/m)	B_{peak}/mT
$\lambda/4$	80.5	1	9.7	17
$3\lambda/4$	201	1	8.06	33.8
$5\lambda/4$	356	1	6.4	32.9

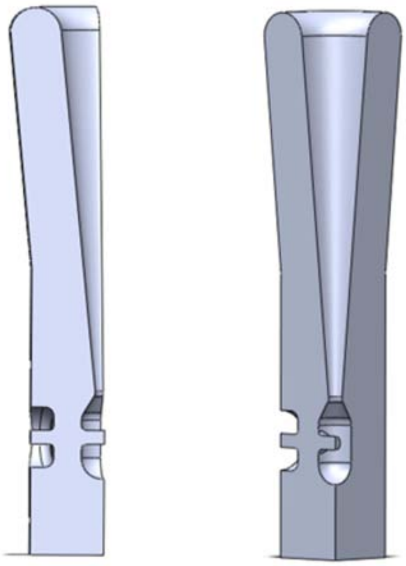

Fig. 1. Schematic of a quarter of the frequency 80.5 MHz, beta 0.085 superconducting tapered QWR.

peak surface magnetic field-B_{peak}. The electric and magnetic field distributions of the three modes are obtained using Analyst 3D eigenmode analysis type [2], based on the geometric symmetry, only a quarter of the cavity was used for the electromagnetic simulation (Fig. 1). Some important electromagnetic figures of merit are shown in Table 1.

3 MP simulations by using Analyst 3D particle tracking (PT3P) [3]

Half of the QWR needs to be used in the MP simulation (Fig. 2). In the PT3P simulation, the geometry is divided into two parts: the top part and the bottom part, in the consideration of the cavity structure and the computations.

In the simulation, it is assumed that the secondary emission yield (SEY) is governed only by a simple relation that is purely a function of impact energy; moreover, the SEY depends strongly on the condition of the cavity inner surface, the SEY of niobium (Nb) is used as: the max secondary emission coefficient $\delta p\approx 1.3$, corresponding to the impact energy of K_{p}=430 eV and the points at which the secondary emission yield passes through one denoted by the first crossover $K_1\approx 130$ eV and the second crossover $K_2\approx 1000$ eV [3] (Fig. 3). The field level was scanned up to 56 MV/m of peak electric field magnitude with a 0.4 MV/m interval, 2 eV emitted kinetic energy, 5° phase increment and 50 RF periods the MP simulation were carried out for each part of the tapered QWR cavity.

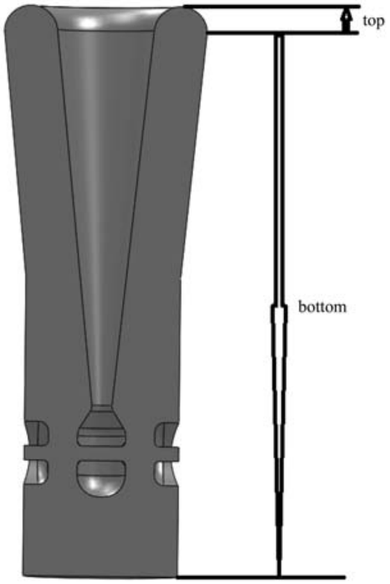

Fig. 2. Two regions for primary particles.

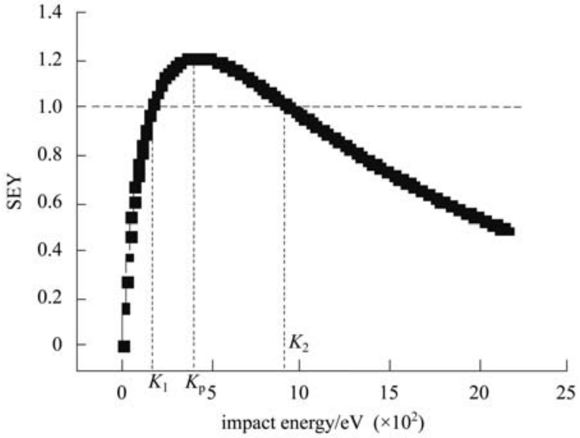

Fig. 3. Generic dependence of SEY on impact energy.

3.1 MP simulation for the fundamental mode ($\lambda/4$ mode)

Electron resonant trajectories were found at the shorting plate, Fig. 4(a) shows how the normalized counter function (NCF) values of different impact numbers change with the electric field magnitude, where NCF is described as the fraction of particles that experience the least n impacts. With the increase of electron impact, NCF drops enormously, which implies a very unstable resonant trajectory. Any field level for a yield function greater than unity indicates a potential multipactor (Fig. 4(b)), there are still resonant trajectories at the short plate at peak electric field levels from 12 to 20.8 MV/m even with 100 impacts. However, to confirm the severity of the occurrence, 100 impacts with an enhanced counter function greater than or equal to 10^5 was adopted as a significant MP level, see Fig. 5(a), and the relevant peak electric field range is from 12.4 to 15.6 MV/m. These are of two-point first-order MP. The impact energies of these trajectories are from 150 to 325 eV (Fig. 5(b)). Since 93% of the resonant particles with yield >1 have impact energies below 250 eV, which are far from the peak SEY for niobium, such a MP band can normally be processed without much difficulty. Furthermore, when the simulation was continued for more than 100 electron impacts, the enhanced counter function decreased dramatically, at 500 impacts, the enhanced counter reduced to zero, indicating a not intense and not stable electron cloud in the cavity.

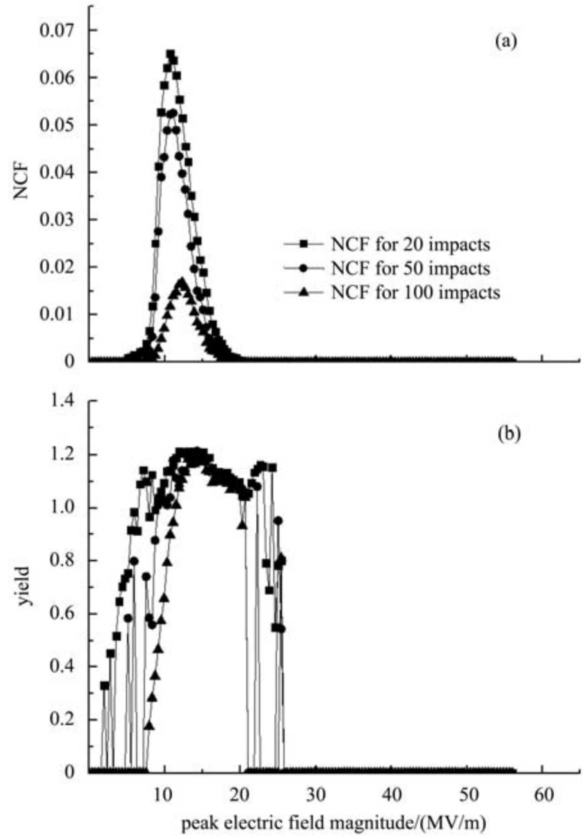

Fig. 4. The normalized counter function (a) and the yield function (b) vs. peak electric field magnitude for 20 impacts, 50 impacts, and 100 impacts, separately.

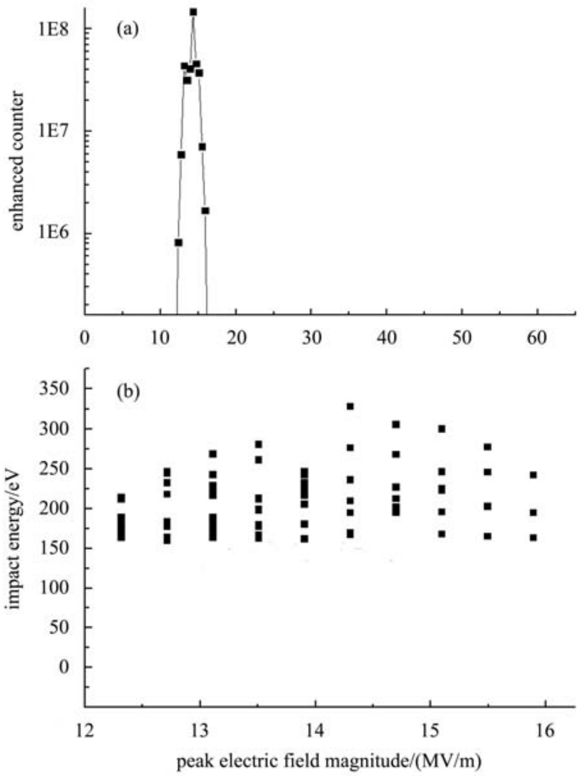

Fig. 5. The enhanced counter function vs. the peak electric field for 100 impacts (a); the impact energy distribution of the trajectories with 100 impacts (b).

3.2 MP simulation for the higher modes ($3\lambda/4$ and $5\lambda/4$ modes)

The simulation results for the higher modes indicate a band of possible MP within which the yield function value is greater than unity for 100 impacts: 16.8–40.4 MV/m for the $3\lambda/4$ mode and 22.4–54.4 MV/m for the $5\lambda/4$ mode, both at the shorting plate (Fig. 6), which is wider than the relevant range for the $\lambda/4$ mode. Similarly, we are more interested in the band range whose enhanced counter function with 100 impacts is greater than 10^5 (Fig. 7), then the dangerous band falls in 18–37.6 MV/m for the

$3\lambda/4$ mode and 22.8–52.4 MV/m for the $5\lambda/4$ mode, and the impact energy distribution in the corresponding range is presented (Fig. 8). For both of the two higher modes, the impact energies range from 150 to 1000 eV, which are across the whole zone for SEY greater than unity. These resonant conditions could potentially present significant MP. Obviously, the MP band in the higher modes is severer than that in the fundamental mode.

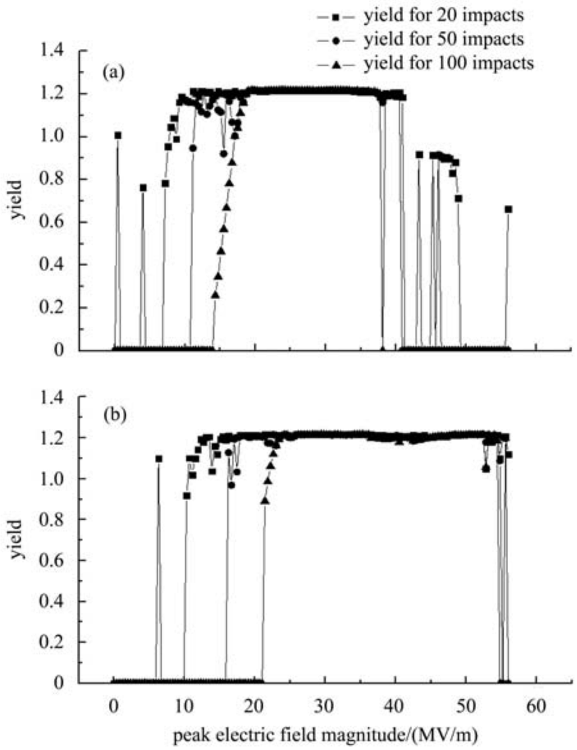

Fig. 6. The yield function of MP for the higher modes; (a): yield vs. peak electric field for the $3\lambda/4$ mode with 20 impacts, 50 impacts, and 100 impacts, separately; (b): yield vs. peak electric field for the $5\lambda/4$ mode with 20 impacts, 50 impacts and 100 impacts, separately.

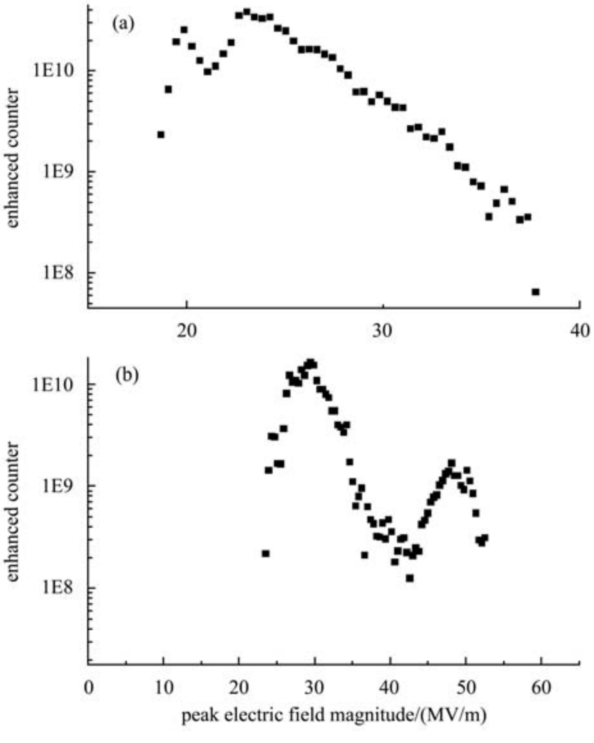

Fig. 7. The enhanced counter function vs. the peak electric field with 100 impacts ((a) for $3\lambda/4$ mode, and (b) for $5\lambda/4$ mode).

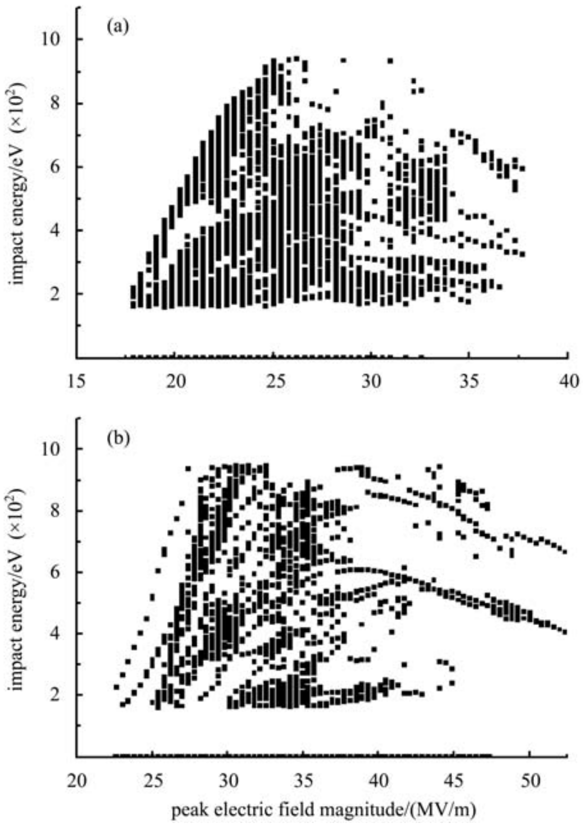

Fig. 8. The impact energy distribution vs. peak electric field with 100 impacts ((a) for $3\lambda/4$ mode, and (b) for $5\lambda/4$ mode).

Comparing the MP situations of the three modes, we can see that the MP bands shift towards a higher electric field range with the change from $\lambda/4$ to $5\lambda/4$ mode; of the three modes, the MP phenomenon in the $3\lambda/4$ mode is the most dangerous one: the enhanced counter functions shown in Fig. 5 and Fig. 7 reveal that the enhanced counter value of the $3\lambda/4$ mode is the largest, and the $3\lambda/4$ mode has the maximum particle proportion, which is located around the peak SEY region. Therefore, it is necessary to do make some fine corrections to the shape of the cavity if higher mode measurement is needed in the vertical tests, and more attention should be paid to the $3\lambda/4$ mode.

4 Conclusion

ANALYST-Particle Tracking was used to analyze the MP bands in the tapered QWR cavity. MP trajectories have been found in the shorting plate region for all of the three modes, however, no obvious resonant trajectories are found in the bottom part of the cavity. In the fundamental mode, the simulations indicate a soft MP barrier at low field, but predict no hard barriers; however, as for the higher modes, hard MP bands are observed through a broad electric field magnitude extent. Thus, we have to make some amendments to certain parts of the cavity if needed, especially with regard to the $3\lambda/4$ mode. Since the cavity will be equipped with couplers and dampers, which are omitted in the simulation, a further complete simulation is going to be carried out.

One of the authors, Zhang Cong, has been in the National Superconducting Cyclotron Laboratory of Michigan State University as a graduate student visitor for half a year and the work of this paper was done there, so she would like to express her sincere thanks to the physicists and engineers of the SRF group at the NSCL for their valuable suggestions and great help.

References

1 Hansan Padamsee, Jens Knobloch, Tom Hays. RF Superconductivity for Accelerators. New York: A Wiley-Interscience Publication, 1998. 179

2 Ostroumov P N, Fuerst J D, Kelly M P, Mustapha B, Shepard K W, XU J. A New ATLAS Efficiency and Intensity Upgrade Project. In: 14th International Conference on RF Superconductivity. Berlin. 2009

3 ANALYST, AWR corporation, El Segundo CA, www.awrcorp.com/analyst